

Depth-Averaged Turbulent Flow Simulation By The Improved Method of Moments

Paik Joongcheol¹⁾ and Cho Woncheol²⁾

1. Introduction

In many environmental applications shallow water turbulence is commonly observed because flows in river, estuary and coastal areas are mainly categorized as shallow water flows in which the horizontal scale of flow geometry is much larger than the vertical scale. In this condition, the flow is well mixed over the water depth due to strong vertical mixing induced by the bottom shear stresses. Consequently, the vertical variation of the mean flow is approximately uniform in the vertical direction. In this case, depth-averaged models have been frequently applied to free surface hydraulic engineering problems because of their efficiency and reasonable accuracy.

The particular physical attributes of real system make some important demands on the numerical methods used for their simulations. Numerical stability, solution accuracy, computational efficiency, and ease of programming are viewed as being crucial factors in the development of an effective numerical method. Overcoming the stability limitation on the time step allows significant improvements in computational efficiency. Furthermore, the computational accuracy may be improved, because the numerical method is used on fewer occasions for any given problem.

The objective of this study is to present an efficient and accurate numerical method to compute turbulent flow in shallow water region. The governing equations are solved in a partially staggered grid system by the fractional step implicit method. The present model consists of three-step computational procedure for momentum quantities and two-step for scalar quantities. The advection of momentum and scalar quantities is computed using the improved method of moments. The diffusion of momentum and scalar quantities and hydrostatic propagation are computed using the implicit finite difference schemes.

2. Depth-averaged Flow Governing Equations

The governing equations used in the present hydrodynamic model in Cartesian coordinates, can be described by the following shallow water equation based on the depth-integrated form of the Reynolds equation for the statistical average of a turbulent flow. The depth-integrated mass conservation and for a constant density turbulent flow on a rotating earth the depth-integrated momentum equations for flow in the horizontal coordinate directions x and y , can be expressed, respectively, as

.....
Post-Doc¹⁾ & Professor²⁾, Department of Civil, Urban & Architectural Engineering, College of Engineering, Yonsei University.

$$\frac{\partial \zeta}{\partial t} + \frac{\partial q_x}{\partial x} + \frac{\partial q_y}{\partial y} = 0 \quad (1)$$

$$\frac{\partial q_x}{\partial t} + \left(\frac{\partial U q_x}{\partial x} + \frac{\partial V q_x}{\partial y} \right) - f q_x + g H \frac{\partial \zeta}{\partial x} + c_f U U_s - \frac{\rho_a}{\rho} c_w W_x W_s - H \left[\frac{\partial}{\partial x} \left(v_h \frac{\partial U}{\partial x} \right) + \frac{\partial}{\partial y} \left(v_h \frac{\partial U}{\partial y} \right) \right] = 0 \quad (2)$$

$$\frac{\partial q_y}{\partial t} + \left(\frac{\partial V q_x}{\partial x} + \frac{\partial V q_y}{\partial y} \right) + f q_x + g H \frac{\partial \zeta}{\partial x} + c_f V U_s - \frac{\rho_a}{\rho} c_w W_y W_s - H \left[\frac{\partial}{\partial x} \left(v_h \frac{\partial V}{\partial x} \right) + \frac{\partial}{\partial y} \left(v_h \frac{\partial V}{\partial y} \right) \right] = 0 \quad (3)$$

1 2 3 4 5 6 7

where ζ = water elevation, H = water depth, unit discharge $q_x = UH$, $q_y = VH$, f = Coriolis parameter, g = acceleration due to gravity, c_f = flow resistance coefficient, c_w = wind resistance coefficient, ρ_a = air density, wind speed $W_s = \sqrt{W_x^2 + W_y^2}$, flow speed $U_s = \sqrt{U^2 + V^2}$, effective viscosity $v_h = \nu + \nu_t$. In (3.34), the various terms are the depth-integral local acceleration (term 1), advective acceleration (term 2), Coriolis force (term 3), pressure gradient (term 4), bed shear resistance (term 5), wind shear force (term 6), and turbulent induced shear force (term 7).

For the closure of the system of equations, the most frequently used model is a single-length-scale two-equation $k - \varepsilon$ model introduced by Rastogi and Rodi (1978). If the flow quantities, such as H , U , and V , satisfy the equation of depth-averaged mass conservation, the variation of k and ε is determined by the numerical solutions of the following depth-averaged transport equations:

$$\frac{\partial k}{\partial t} + U \frac{\partial k}{\partial x} + V \frac{\partial k}{\partial y} = \frac{1}{H} \frac{\partial}{\partial x} \left(\frac{v_t H}{\sigma_k} \frac{\partial k}{\partial x} \right) + \frac{1}{H} \frac{\partial}{\partial y} \left(\frac{v_t H}{\sigma_k} \frac{\partial k}{\partial y} \right) + P - \varepsilon + P_{kv} \quad (4)$$

$$\frac{\partial \varepsilon}{\partial t} + U \frac{\partial \varepsilon}{\partial x} + V \frac{\partial \varepsilon}{\partial y} = \frac{1}{H} \frac{\partial}{\partial x} \left(\frac{v_t H}{\sigma_\varepsilon} \frac{\partial \varepsilon}{\partial x} \right) + \frac{1}{H} \frac{\partial}{\partial y} \left(\frac{v_t H}{\sigma_\varepsilon} \frac{\partial \varepsilon}{\partial y} \right) + c_{1\varepsilon} \frac{\varepsilon}{k} P - c_{2\varepsilon} \frac{\varepsilon^2}{k} + P_{\varepsilon v} \quad (5)$$

where the term for the turbulence energy production due to the horizontal shear is

$$P = v_t \left[2 \left(\frac{\partial U}{\partial x} \right)^2 + 2 \left(\frac{\partial V}{\partial y} \right)^2 + \left(\frac{\partial U}{\partial y} + \frac{\partial V}{\partial x} \right)^2 \right] \quad (6)$$

The terms originating from non-uniformity of vertical profiles are assumed to be absorbed in the product terms P_{kv} and $P_{\varepsilon v}$. The standard values for the model parameters are $c_{1\varepsilon} = 1.44$, $c_{2\varepsilon} = 1.92$, $c_k = 1.0$, and $c_\varepsilon = 1.3$. These constants have been chosen to make the model compatible with the logarithmic velocity distribution near the wall with $\kappa = 0.435$. Eqs. (2)–(5) can be written in a general form of a balance of convection, diffusion, and product terms

$$\frac{\partial \phi}{\partial t} + U \frac{\partial \phi}{\partial x} + V \frac{\partial \phi}{\partial y} = \frac{1}{H} \left[\frac{\partial}{\partial x} \left(H \Gamma_{x11} \frac{\partial \phi}{\partial x} \right) + \frac{\partial}{\partial y} \left(H \Gamma_{y22} \frac{\partial \phi}{\partial y} \right) \right] + S_\phi \quad (7)$$

The symbolic variables of ϕ , Γ , and in (7) for the momentum and turbulence transport equations can be expressed as:

For the momentum equation

$$\phi = U, \quad \Gamma_{u11} = \nu_t / \sigma_k + \nu, \quad \Gamma_{u22} = \Gamma_{u11}, \quad S_u = -gH(\partial\zeta/\partial x) - c_f UU_s \quad (8)$$

$$\phi = U, \quad \phi = V, \quad \Gamma_{v11} = \nu_t / \sigma_k + \nu, \quad \Gamma_{v22} = \Gamma_{v11}, \quad S_v = -gH(\partial\zeta/\partial y) - c_f VU_s \quad (9)$$

For kinematic turbulence energy and its dissipation rate

$$\phi = k, \quad \Gamma_{k11} = \nu_t / \sigma_k + \nu, \quad \Gamma_{k22} = \Gamma_{k11}, \quad S_k = P - \varepsilon + P_{kv} \quad (10)$$

$$\phi = \varepsilon, \quad \Gamma_{\varepsilon 11} = \nu_t / \sigma_\varepsilon + \nu, \quad \Gamma_{\varepsilon 22} = \Gamma_{\varepsilon 11}, \quad S_\varepsilon = c_{1\varepsilon} \frac{\varepsilon}{k} - c_{2\varepsilon} \frac{\varepsilon^2}{k} + P\varepsilon v \quad (11)$$

3. Solution method

The present chapter introduces an implicit fractional three-step method to solve the depth-averaged shallow water equation. This procedure is based mainly on the principle of the split-operator approach proposed by Benque et al. (1982). Substituting $q_x = UH$ and $q_y = VH$ and assuming that U , V , and H satisfy the continuity equation, advection equation (7) can be written as

$$\frac{\phi^{n+1/3} - \phi^n}{\Delta t} + U^n \frac{\partial \phi^n}{\partial x} + V^n \frac{\partial \phi^n}{\partial y} = 0 \quad (12)$$

Once $\phi^{n+1/3} = U^{n+1/3}$ or $V^{n+1/3}$ is computed by using (12), the corresponding unit discharges are determined using $q_x = U^{n+1/3} \cdot H^n$ and $q_y = V^{n+1/3} \cdot H^n$.

The diffusion operator can be expressed as

$$\frac{\phi^{n+2/3} - \phi^{n+1/3}}{\Delta t} = H \frac{\partial}{\partial x} \left(\Gamma_{11} \frac{\partial \phi^{n+1/3}}{\partial x} \right) + H \frac{\partial}{\partial y} \left(\Gamma_{22} \frac{\partial \phi^{n+1/3}}{\partial y} \right) + S_\phi \quad (13)$$

The hydrostatic propagation step combines the continuity equation with the remainder of the momentum equations.

$$\frac{\zeta^{n+1} - \zeta^n}{\Delta t} + \left(\frac{\partial q_x}{\partial x} + \frac{\partial h_1 q_y}{\partial y} \right) = 0 \quad (14)$$

$$\frac{q_x^{n+1} - q_x^{n+2/3}}{\Delta t} + g \left(H \frac{\partial \zeta}{\partial x} \right) + c_f UU_s = 0 \quad (15)$$

$$\frac{q_y^{n+1} - q_y^{n+2/3}}{\Delta t} + g \left(H \frac{\partial \zeta}{\partial y} \right) + c_f VU_s = 0 \quad (16)$$

The bed friction is a function of water depth and flow velocity, which can be expressed as:

$$c_f UU_s = g q_\zeta^{n+1} q_s^{n+2/3} / (C_z^{n+2/3} H^n)^2 \quad (17)$$

where $q_s = \sqrt{(q_\xi^{n+2/3})^2 + (q_\eta^{n+2/3})^2}$. Substituting the bed friction term (17) into (15), the expression of momentum quantities at time level $n+1$ can be represented as follows:

$$q_\xi^{n+1} = \frac{1}{A} q_\xi^{n+2/3} - \alpha_p \frac{g\Delta t H^{n+1}}{Ah_1} \frac{\partial \zeta^{n+1}}{\partial \xi} - (1 - \alpha_p) \frac{g\Delta t H^n}{Ah_1} \frac{\partial \zeta^n}{\partial \xi} \quad (18)$$

where $A = 1 + g\Delta t q_s^{n+2/3} / (C_z^{n+2/3} H^n)^2$. Similarly, (16) can be written in term of q_η^{n+1} . Then, Substituting (18) into (14) and introducing $H^{n+1} = h + \zeta^n + \Delta\zeta$ and $\zeta^{n+1} = \zeta^n + \Delta\zeta$ yields to the equation in the single unknown $\Delta\zeta$

$$\begin{aligned} -\frac{\Delta\zeta}{g\Delta t^2} + \frac{\alpha_p^2}{J} \frac{\partial}{\partial \xi} \left(\frac{h_2 H^n}{h_1 A} \frac{\partial \Delta\zeta}{\partial \xi} + \frac{h_2 \Delta\zeta}{h_1 A} \frac{\partial \zeta^n}{\partial \xi} \right) \\ + \frac{\alpha_p^2}{J} \frac{\partial}{\partial \eta} \left(\frac{h_1 H^n}{h_2 A} \frac{\partial \Delta\zeta}{\partial \eta} + \frac{h_1 \Delta\zeta}{h_2 A} \frac{\partial \zeta^n}{\partial \eta} \right) = -S_\zeta \end{aligned} \quad (19)$$

The governing equations are solved in a partially staggered grid system by the fractional step implicit algorithm. The advection of momentum and scalar quantities is computed using the improved method of moments including a new moment updating procedure (Paik and Cho, 1999). The diffusion of momentum and scalar quantities and the hydrostatic propagation are discretized by the implicit second-order central differencing. This differencing creates a coefficient matrix banded by five diagonal elements. The resulting system of equations is solved iteratively by the strongly implicit procedure (SIP). Stone's method usually converges in a small number of iterations for solving non-linear problems with moderate accuracy (Ferziger and Feric, 1996).

4. Application

The developed numerical model is applied for predicting the tide-induced circulation in narrow entranced rectangular harbor. The subject test has considered the harbor geometry with the dimensions being approximated as closely as possible to those of the laboratory models. Falconer and Yu (1991) conducted a series of experiments for tidal eddies in a rectangular harbor with narrow entrances. The model harbor was set to be square, with prototype dimensions of 432 m × 432 m and was assumed to experience sinusoidal repeated semidiurnal tides of period 12.4 hours and range 4 m, as shown in Fig. 1. The horizontal and vertical scale ratios of hydraulic mode are 1:400 and 1:40, respectively. The computational domain consisted of a mesh of 35 × 28 grid squares. The grid spacing for the simulation is 0.06 m and the time step is 0.4 s. The equivalent sand grain roughness height k_s is 0.05mm. For closed boundaries, the no-slip boundary condition and the wall function were applied. Also the wall function was applied to two computational grid points near the entrance. For the open boundary conditions of the numerical model a sinusoidal tide of period 707 was assigned at the open boundaries. The tidal range and the mean harbor depth are 0.10 m and 0.15 m.

The typical predicted velocity fields by the present model at mean water level flood and ebb tides are shown in Fig. 2. The predicted velocity fields appeared to produce the realistic circulatory velocity fields, particularly, clockwise rotating gyres at mean water level ebb tide. A general comparison of

velocity field predictions did not appear to show a marked difference with those published in recent studies by Falconer and Guiyi (1994). Although no experimental data were available for the eddy viscosity distributions at the time of the study, numerical predictions are obtained of the eddy viscosity distributions at mean water flood and ebb tides shown in Fig. 3. In comparison these figures with those in the previous study (Falconer and Guiyi, 1994), the eddy viscosity values in the vicinity of the harbor entrance appeared to be of similar magnitude. Within the harbor at the mean water level flood tide, however, it can be seen that there is a certain difference in the eddy viscosity magnitudes. This difference is due to advection of the relatively high turbulence generated by the high velocity and shear gradients along the separation streamline near the wall downstream of the harbor entrance. This difference by one order in the magnitude of the eddy viscosity did not give a significant influence on circulation flow pattern (Langerak, 1987). However, this variation has been included in the diffusion process, which may give much significance in mass transport modeling.

5. Conclusions

The present research focuses on the development of the improved method of moments with variance diminishing procedure for solving the advective transport of momentum and scalar quantities. The present numerical method has been successfully applied to predict the tidal induced circulation flow and the steady-state recirculating flow problems with laboratory flume data. Comparisons of the numerical solutions with the published experimental results have demonstrated that the present numerical method produces the encouraging accuracy and can be applied to real problems with various dynamic and geometric boundary conditions.

6. References

- Benqué, J.P., Cunge, J.A., Fuillet, J., Hauguel, A., and Holly, F.M. (1982). "New method of tidal current computation." *J. Wtrwy., Port, Coast., and Oc. Div.*, ASCE, 108(3), 396-417.
- Falconer, R.A. and Guiyi, L. (1994). "Numerical modeling of tidal eddies in coastal basins with narrow entrance using the $k - \epsilon$ turbulence model." *Mixing and transport in the environment*, K.J. Beven, P.C. Chatwin, and J.H. Millbank, eds, John Wiley & Sons Ltd., Chichester, England.
- Falconer, R.A. and Yu, G.P. (1991). "Effects of depth, bed slope and scaling on tidal currents and exchange in a laboratory model harbor." *Proc. Inst. Civ. Engin. Part 2, Res, Theory 91*, 561-576.
- Ferziger, J.H. and Peric, M. (1996). *Computational methods for fluid dynamics*, Springer, Berlin.
- Langerak, A. (1987). "Secondary currents and their influence on depth-averaged tidal models." *Proc., XXII Congr. of IAHR, Technical Session B*, Lausanne, Switzerland, 65-70.
- Paik, J.C. and Cho, W. (1999). "Accurate variance diminishing procedure in method of moments for advection simulation.", *J. Civil Engrg.*, KSCE, 3(4), 359-368.
- Rastogi, A.K. and Rodi, W. (1978). "Predictions of heat and mass transfer in open channels." *J. Hydr. Engrg.*, ASCE, 104(3), 397-420.

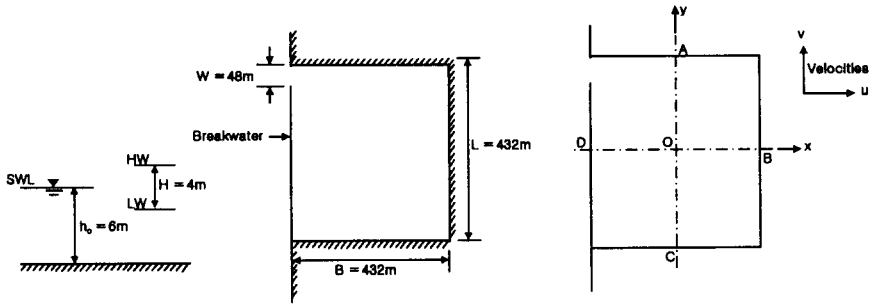


Fig. Prototype harbor dimensions and coordinate system

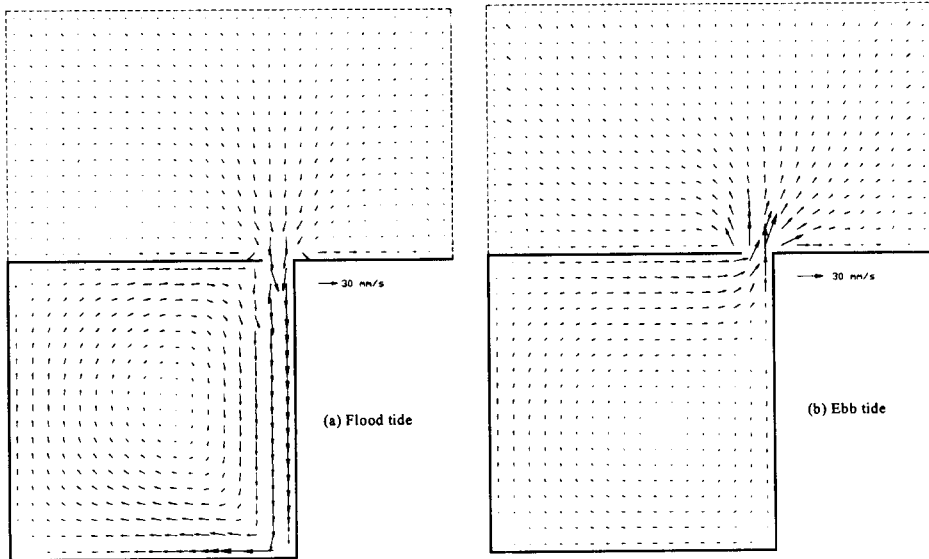


Fig. 2. Predicted velocity field at mean water level flood and Ebb tides

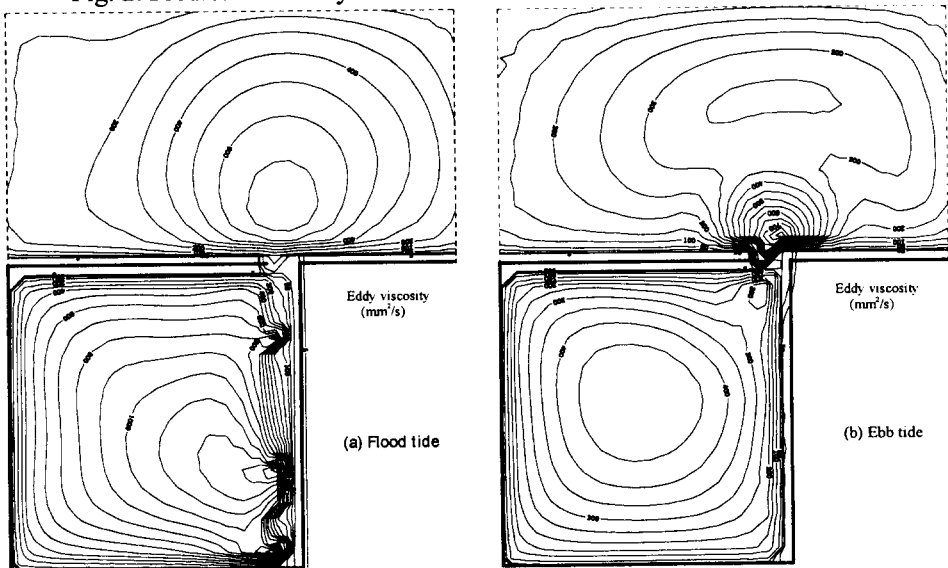


Fig. 3 Isolines of predicted eddy viscosity at mean water level flood and ebb tides